Journal of Statistical Physics, Vol. 63, Nos. 3/4, 1991

Cluster Growth in Particle-Conserving Cellular Automata

Tamotsu Kohyama[1]

Received October 8, 1990; final December 10, 1990

A class of simple two-dimensional cellular automata with particle conservation is proposed for easy simulations of interacting particle systems. The automata are defined by the exchange of states of neighboring cells, depending on the configurations around the cells. By attributing an energy to a configuration of cells, we can select significant rules from the huge number of possible rules and classify them into several groups, based on the analogy with a binary alloy. By numerical calculations, cluster growth is found in two kinds of phases which reveal gas–solid coexistence and liquid droplets. Normalized scaling functions are obtained, and dynamical scaling is examined.

KEY WORDS: Cellular automata; particle conservation; clusters; spinodal decomposition; dynamical scaling.

1. INTRODUCTION

To investigate complex dynamical systems numerically, Monte Carlo and molecular dynamics methods are usually used. But in recent years cellular automata (CA)[1] have been adopted more and more as another method.[1,2] Several CA models have been developed for simulations of fluids[3] and for lattice models like the Ising[2,4] and Potts[5] models. Problems of ergodicity were studied by reversible CA.[6] Since CA are discrete in time, space and state, it is difficult to construct models which correspond directly to real physical systems. But as the number of possible CA is huge, one can expect to find rules to correspond to most real systems. Once a good rule is found, we can use it as an efficient simulation method. From another point of view, CA can be used as "mind stretchers"

[1] Faculty of Education, Shiga University, Otsu 520, Japan.

0022-4715/91/0500-0637$06.50/0

which show complex phenomena that are seen in the real world, but are often assumed to require much more input structure.

One of the most interesting problems is the pattern dynamics in systems with many particles interacting by short-range couplings. Previously we had studied a one-dimensional CA model[7] for such systems. In this paper we will extend it to the two-dimensional case with particle conservation, and study several aspects of pattern growth as a model of spinodal decomposition (a similar model[8] was studied recently). We show that rules with physically realistic behavior exist, and find two types of cluster growth which remind us of gas–solid coexistence and liquid droplet formation.

In Section 2, we explain and classify the CA studied in this paper. They are a subset of those CA which can be interpreted as systems of conserved particles on a two-dimensional lattice. Section 3 shows the results of numerical simulations. To characterize the evolution with time, we define two quantities: the mean density n_{10} of particle–hole pairs, and the density v of sites which change at one time step. By studying them in detail, including their scaling properties, we show that there are at least two types of growth. The mechanism of cluster growth is summarized in Section 4.

2. PARTICLE-CONSERVING CA

2.1. Elementary Processes

Extending the previous one-dimensional case, we consider a 2d square lattice on which the variables s_j take only two values $s_j = 0$ or $s_j = 1$. As the only elementary process, we assume that two neighboring sites can exchange their states. Thus the total "spin" $\sum_j s_j$ is conserved as in Kawasaki's[9] Ising model. This exchange is done deterministically, depending only on the pair and the configuration of the six sites surrounding the pair. Without restriction on the kind of rule, there would be the tremendous number of 2^{64} rules. We reduce this by attributing an energy to each of the six bonds linking the pair with its six neighbors, and performing the exchange iff the total energy is above a certain threshold E_*. This is the main difference with respect to Monte Carlo simulations, where flips are decided statistically, on the basis of energy differences or on the basis of the energy of the final state.

Without restricting generality, we can assume the energy of a pair '10' to be zero, and the energy threshold to be

$$E_* = \pm 1$$

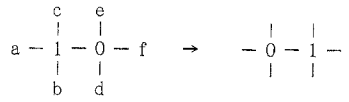

Fig. 1. Configuration around the pair '10' where a, b, c, d, and e are 0 or 1. If ΔE defined by Eq. (1) is greater than 0, the '10' pair updates to '01'.

The energies of '00' and '11' pairs are called E_0 and E_1, respectively. Consider a central pair '10' as in Fig. 1 (for a central pair '01' the arguments are completely analogous; central pairs '00' and '11' need not considered anyhow), and denote by α the sum of 'up' neighbors of the left spin, and by β the sum of 'up' neighbors of the right spin, i.e., this configuration is denoted by (α, β). Then the pair is exchanged if and only if

$$\Delta E = \alpha E_1 + (3 - \beta) E_0 - E_* > 0 \tag{1}$$

2.2. Coding and Classifying the Rules

The easiest way to visualize each possible rule is graphically. If we represent each possible neighborhood of a '10' pair by a point on a 4×4 lattice with coordinates (α, β), then Eq. (1) defines a straight line separating lattice points with $\Delta E > 0$ from points with $\Delta E < 0$ (see Fig. 2). Each straight line (i.e., each rule) separates the 16 possible neighborhoods into two groups, one of which leads to an exchange and the other does not.

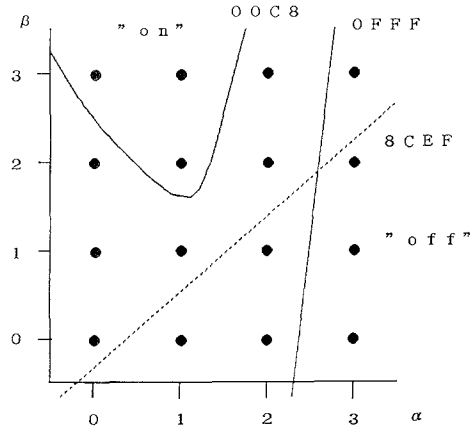

Fig. 2. Each straight line dividing the 16 points of this lattice into two groups of "on" ($\Delta E > 0$) and "off" ($\Delta E < 0$) points corresponds to a CA rule. When $E_1 < 0$ and $E_2 < 0$, the full line corresponds thus to $N_{\text{rule}} = 0\text{FFF}$, while the dashed line is $N_{\text{rule}} = 8\text{CEF}$.

We can thus encode each rule by a number N_{rule} between 0 and $2^{16}-1$, where the kth binary digit is 1 iff the configuration (α, β) with $\alpha = [k/4]$, $\beta = (k \bmod 4)$ leads to an exchange. In the following, N_{rule} will always be written as a four-digit hexadecimal number. For instance, FFFF is $2^{16}-1$, and 0000 is 0. As an example of the encoding, we take the rule represented by the full line in Fig. 2, whose code N_{rule} is 0FFF. The full line separates the configurations $(3, \beta)$ (where $\beta = 0, 1, 2, 3$) with $\Delta E < 0$ from the configurations with $\Delta E > 0$. This implies that the $(3 \times 4 + \beta)$th binary digit of N_{rule} is 0 and the other digits are 1, i.e., the binary code is 0000111111111111 and the hexadecimal code is 0FFF.

It is obvious from the geometrical construction that only a tiny fraction of all 2^{16} rule numbers correspond to allowed rules (the others correspond to divisions by curved lines in Fig. 2). By an exhaustive search, we found altogether 174 allowed rules.

If we interpret the system as a lattice gas, with $s = 1$ being a particle and $s = 0$ an empty place, then Fig. 3a corresponds to an isolated particle surrounded by vacuum, while Fig. 3b corresponds to an isolated hole.

Assume that the hole in Fig. 3a has the same number of hole neighbors as the particle in Fig. 3b has particle neighbors, $a+b+c = 3-d-e-f$. Then, the isolated particle in Fig. 3a has a bigger (smaller) energy than the isolated hole in Fig. 3b if $E_0 > E_1$ ($E_0 < E_1$). Thus, if $E_0 > E_1$, then the dominant mechanism is the hopping of particles, while the mobility of holes is larger if $E_0 < E_1$.

Another classification is based on the analogy with a binary alloy, with $s_j = 0$ and $s_j = 1$ representing the two atoms A and B. If $E_0 + E_1 < 0$, then atoms of the same kind are more tightly bound and tend to cluster as in a eutectic alloy. In the inverse case $E_0 + E_1 > 0$, the system behaves like a solution since different atoms tend to mix.

Using $E_m = (E_0 + E_1)/2$, this leads to a classification into eight groups, if we distinguish in addition by the strength of the particle–hole asymmetry. This is summarized in Table I.

We should point out that this is a classification of maps neighborhood → energy. It is not a mutually exclusive classification of CA rules. For instance, rule FFFF (always exchange) can arise from all classes when $E_* = -1$.

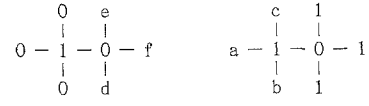

Fig. 3. Configuration (a) indicates an isolated particle and (b) an isolated hole corresponding to (a), where $a = 1-f$, $b = 1-d$, and $c = 1-e$.

Table I

	Eutectic alloy	Solution
Particle	$E_1 < E_m < 0$; I: $E_0 > 0$	$E_1 > E_m > 0$; V: $E_0 < 0$
	II: $E_0 < 0$	VI: $E_0 > 0$
Hole	$E_0 < E_m < 0$; III: $E_1 < 0$	$E_0 > E_m > 0$; VII: $E_1 > 0$
	IV: $E_1 > 0$	VIII: $E_1 < 0$

2.3. Dynamics

Though we have defined above the rules for updating each pair, we have not yet mentioned how we select the pairs in the two-dimensional lattice space. One possible way to select them is random, where the pair to be updated is asynchronously and randomly selected. However, in what follows we adopt synchronous and deterministic dynamics.

In our synchronous dynamics, one time step consists of four processes, which are described in Figs. 4a and 4b. Under these dynamics each site can interact with every nearest neighbor site in two time steps. With these dynamics, a free particle described by the FFFF code moves along the

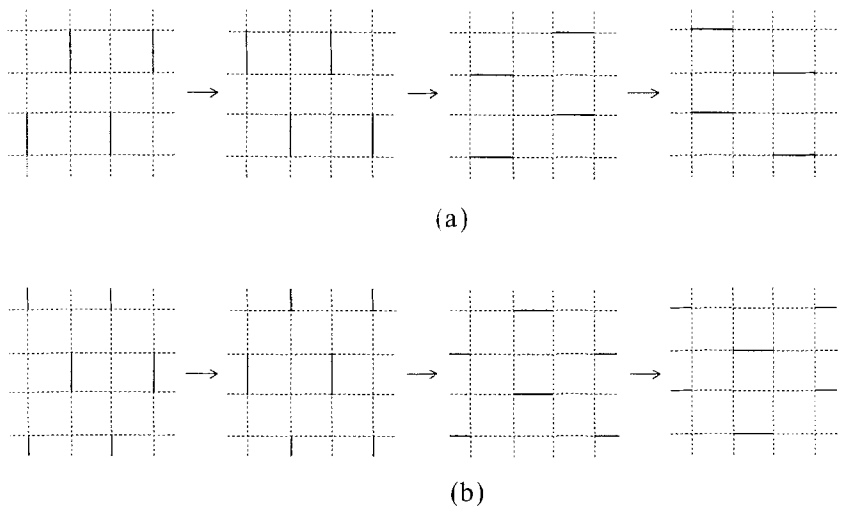

Fig. 4. (a) Four processes of updating which constitute one time step. Two neighboring sites connected by a solid line indicate the pairs to be updated according to the elementary rule. (b) The next time step to part (a). The origin of the pattern (a) is shifted to the coordinate (1, 1).

diagonal direction one lattice spacing per one time step even if two such particles happen to collide. Therefore this system is not mixing. If we consider more complex dynamics, the mixing property[10] can be recovered, but the details are not studied in this paper.

3. NUMERICAL EXPERIMENTS

3.1. Examples

We will show numerical experiments for several rules, concentrating on the eutectic alloy-like phase in the groups I and II, with $E_* = -1$.

As the main observables we measure the density n_{10} of '10' pairs (measured per lattice site, i.e., $n_{00} + n_{10} + n_{11} = 2$), and the density v of sites

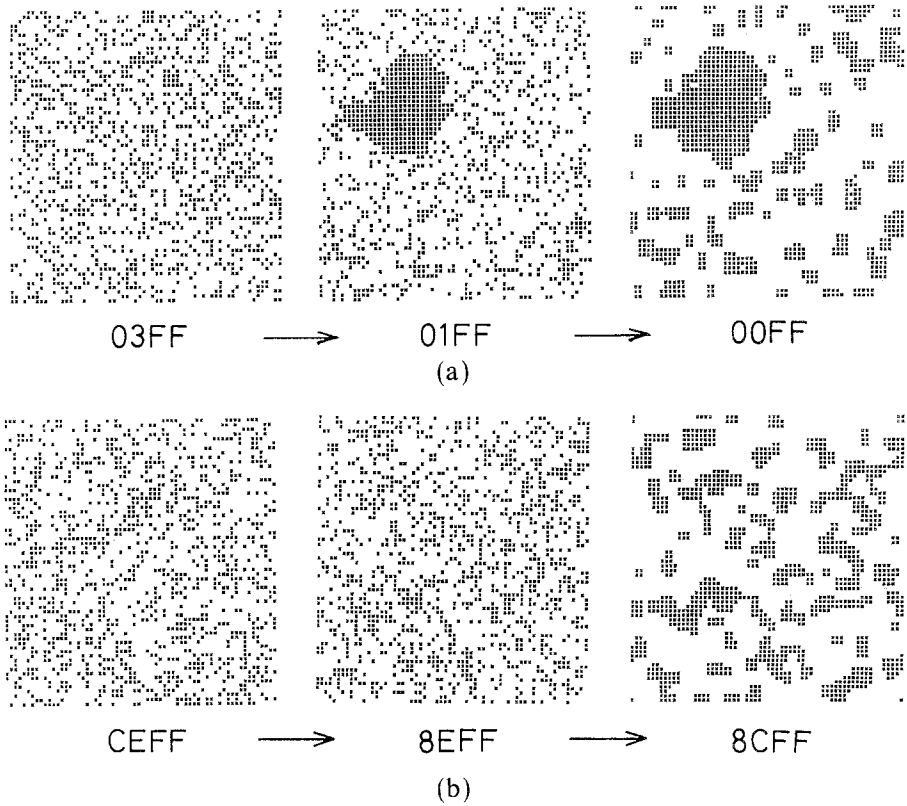

Fig. 5. Typical examples of patterns generated sequentially when E_1 and E_0 are decreased. Dots indicate state 1. Concentration of '1' sites is 0.3. (a, b) Groups I and II, respectively, defined in Section 2.2. The hexadecimal numbers under the patterns are the codes of rules.

which change state at one time step. The quantity v describes the activity or 'softness' of the system.

The total energy of the system can be written as

$$E = N(n_{11}E_1 + n_{00}E_0) = 2N[(1-c)E_0 + cE_1] - Nn_{10}E_m \qquad (2)$$

where N is the total number of sites and c is the concentration of '1' sites, $c = 1/N\sum_j s_j$. We have used the relation $2c = n_{11} + n_{10}/2$.

To observe the appearance of order, we slowly decrease the energy of the system initially obeying rule FFFF. This procedure corresponds to cooling a gas in a real system, because the behavior of rule FFFF is similar to that of a free gas. In our model the decrease of the energy implies the change of the local rule. For numerical experiments, we initialize the distribution of '1' sites and evolve the system under the rule FFFF. After some time steps, each of the energies E_0 and E_1 is lowered and the rule changes. The updating of sites is continued, until a stationary state is achieved. Then n_{10} and v are evaluated. This procedure is iterated until no excitation (i.e., no change) occurs.

From numerical simulations for classes I and II with $E_* = -1$, we find that the system becomes a solid state from a fluid one as the energies E_0 and E_1 are decreased. Some typical examples of patterns are shown in Fig. 5 and the evaluated n_{10} and v are shown in Fig. 6. These figures

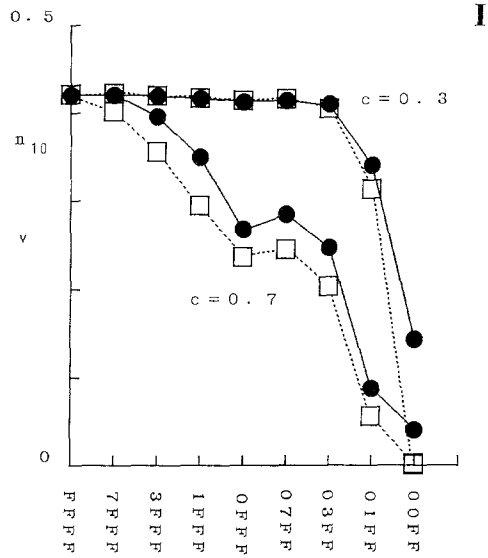

Fig. 6. Examples of two quantities n_{10} and v obtained for the group I when E_1 and E_0 are decreased. Solid circles indicate n_{10} and open squares indicate v. Initial distribution is random with concentration c. The graph is obtained for one subgroup belonging to I.

indicate that the activity v and the number of 1–0 bonds n_{10} decrease as the energies E_0 and E_1 are decreased, i.e., from Eq. (2) and $E_m < 0$, the system tends to develop into a state with lower total energy E.

Viewing Fig. 6, we can find several states with finite v and $n_{10} < 2c(1-c)$, where $2c(1-c)$ is the density of '10' pairs for random distribution. In these states, the system is active, but some ordering can be induced. Two typical rules resulting in such states are 01FF with $c = 0.3$ and 0FFF with $c = 0.7$. As is shown in Fig. 6, the rule 01FF generates a phase which is similar to a gas–solid coexistence system.

From Figs. 5a and 5b, the appearance of the ordered phase is roughly classified into the following routes:

I gas → gas + solid → solid

II gas → solid

3.2. Cluster Growth

As is discussed above, nonperfect ordering with ongoing activity can be found in group I. Thus, we explore the two types of systems given by rules 01FF and 0FFF.

First we study the characteristics of the rule 01FF. The concentration dependences of the quantities n_{10} and v estimated by numerical experiments started from random configurations are shown in Fig. 7. Large deviations

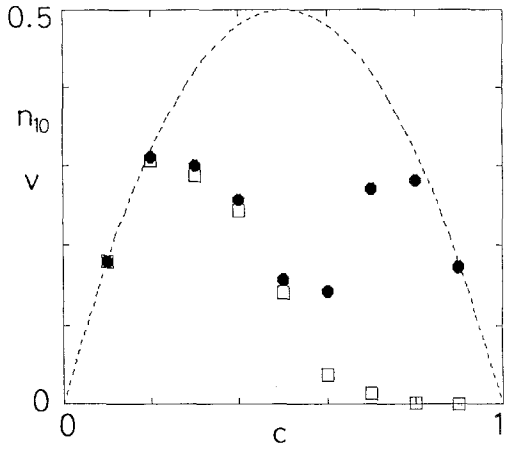

Fig. 7. Concentration dependence of n_{10} and v for the system of code 01FF. Solid octagons indicate n_{10} and open squares indicate v. The broken line represents the two quantities n_{10} and v for a free gas code FFFF. It is given by $2c(1-c)$.

of n_{10} from the value of a free gas system when $0.25 < c < 0.8$ indicate the growth of some kind of order. Since v is positive when $c < 0.8$, the system induces some order with activity when $0.25 < c < 0.8$. Figures 8a and 8b show the temporal behavior of patterns for concentration 0.3 and 0.5. These figures remind us of a gas–solid coexistent state, because there exist large rigid clusters in the sea of many free particles. A large cluster is created after a long time by a complex collision process. The remaining particles outside the dominant cluster are still active, but they cannot make other large clusters. Examining Figs. 8a and 8b, we can say that the characteristics of the growth and the forms of the clusters are different, depending on the concentration. For $0.2 < c < 0.5$, many small clusters appear in early time stages, but only one large cluster dominates after a long time in a finite system. For $0.5 < c$, however, a percolating cluster appears in very early time stages and the cluster deforms from a complex form to a very simple one. The $c = 0.5$ is an approximate threshold level to differentiate

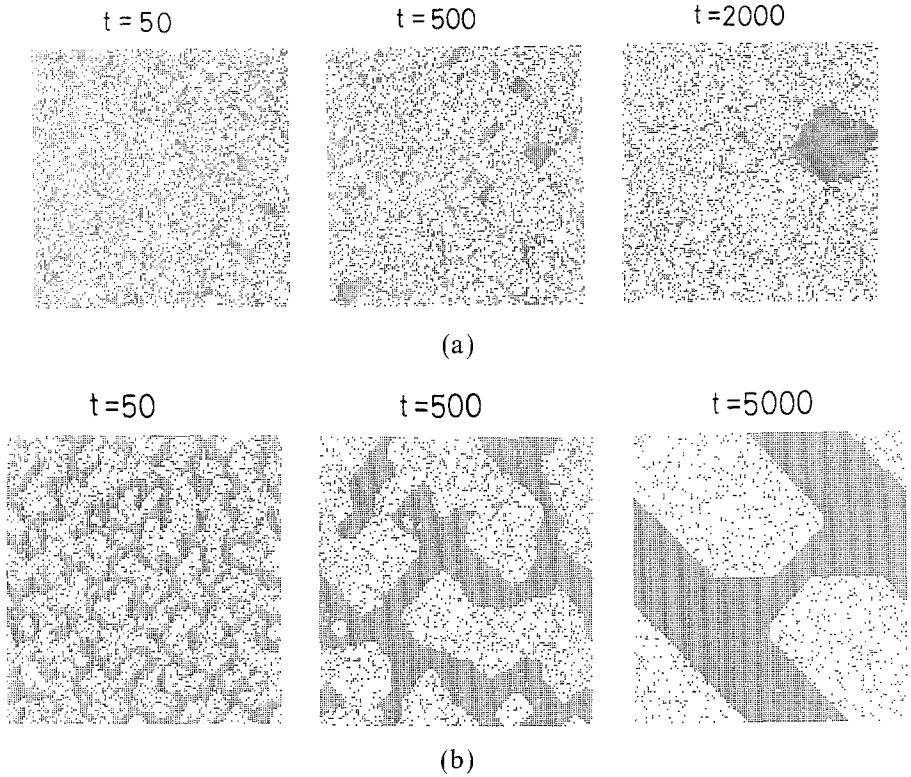

Fig. 8. Pattern change for the system of code 01FF initiated from the random configuration with (a) $c = 0.3$ (b) $c = 0.5$.

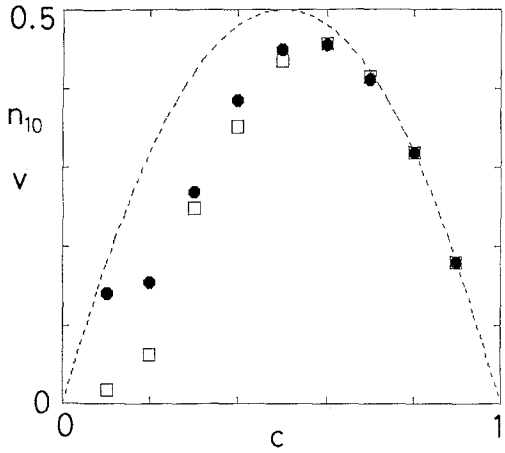

Fig. 9. Concentration dependence of n_{10} and v for the system of code EEEE. Octagons and squares indicate n_{10} and v, respectively. The broken line represents the two quantities for a free gas system.

these two types of cluster growth, but the accurate threshold is not known. In each case the mechanism of cluster growth consists of adhesion and evaporation processes of particles.

Another type of cluster growth is seen under the rule 0FFF with large concentration of '1' sites. Since the system with small c is more easily understood than the system with large c, it is convenient to study the rule EEEE, which is equivalent to 0FFF by the particle–hole symmetry. The two characteristic quantities n_{10} and v are calculated numerically and shown in Fig. 9. We can observe large ordering for $0.1 < c < 0.6$, because n_{10} and v differ largely from those of a free gas state. An example of temporal behavior is shown in Fig. 10 for $c = 0.3$. The figure suggests that the

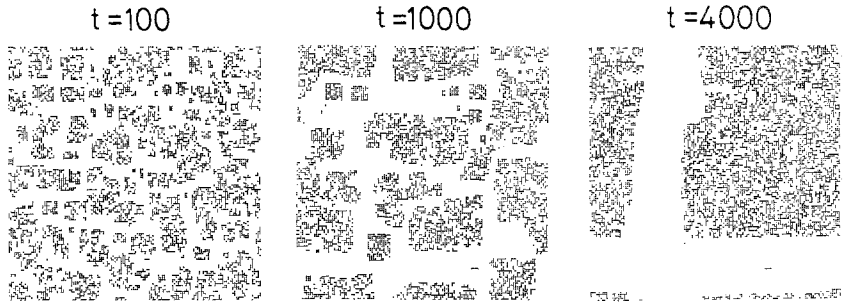

Fig. 10. Pattern change for the system of code EEEE with $c = 0.3$.

mechanism of cluster growth is quite different from that of rule 01FF. Since isolated particles cannot move, the adhesion and evaporation of particles are not significant, but the cluster motion becomes important. Therefore the mechanism of the cluster growth consists of cluster movement, cluster deformation, and cluster–cluster coalescence. These dynamical characteristics remind us of a system with many liquid droplets. Resembling the rule 01FF, there is a critical concentration that separates the two types of cluster distribution, one with a broad distribution of clusters, and the other with very few, very large clusters. The critical concentration is nearly equal to 0.3, but the precise value has not been obtained.

3.3 Scaling Functions

From the patterns of cluster growth obtained in Section 3.2, we can conjecture that dynamical scaling will be satisfied in those clustering processes. We have found numerically that scaling seems indeed to exist in a certain time interval.

The scaling function is derived from consideration of spinodal decomposition.[11] The correlation function is written as

$$C(r, t) = 1/N \sum_i \langle [c(r_i, t) - c][c(r_i + r, t) - c] \rangle \tag{3}$$

where $c(r_i, t)$ is the state value (0 or 1) of the site r_i. The structure function is obtained by the Fourier transformation of the correlation function $C(r, t)$,

$$S(k, t) = \sum_r e^{ikr} C(r, t) = 1/N \left\langle \left| \sum_r e^{ikr} (C(r, t) - c) \right|^2 \right\rangle \tag{4}$$

Since our system is assumed to be isotropic, we reduce the two-dimensional structure function to a one-dimensional one by averaging over the circle of radius $|k|$, i.e.,

$$S(k, t) = \sum' S(k, t) \Big/ \sum' 1 \tag{5}$$

where $\sum'$ is the summation over k which have the same absolute value $|k|$. For numerical calculations, finite-size effects must be taken into account and the structure function must be modified in some degree. We define the modified structure function as follows:

$$S_1(k, t) = S(k, t) - S_{\text{crit}}(k) \qquad \text{for} \quad k_c \tag{6}$$

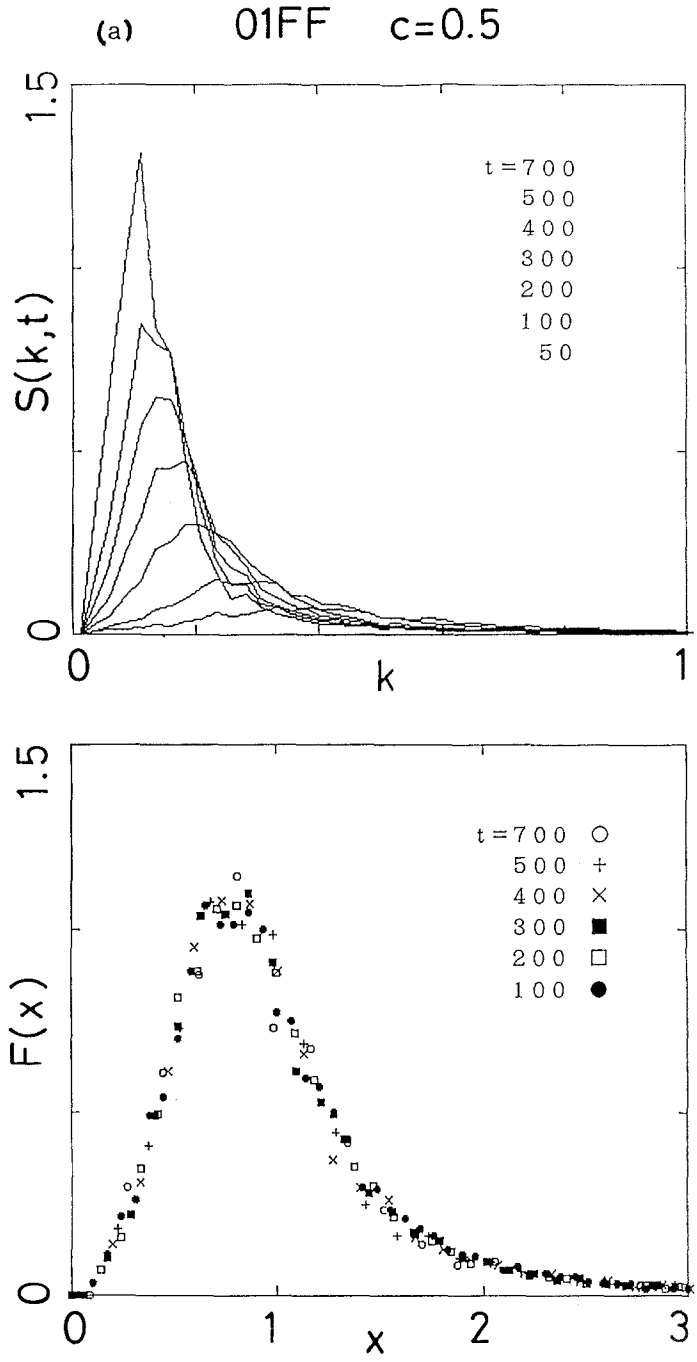

Fig. 11. Structure function $S(k, t)$ and scaling function $F(x)$ obtained numerically. Graphs for several times are superimposed. The rule code and concentration are (a) 01FF, $c=0.5$ and (b) EEEE, $c=0.3$. As $S_{\text{crit}}(k)$, we use the structure function (a) $c=0.22$ and (b) $c=0.65$. The cutoff wave number is $k_c=1.5$.

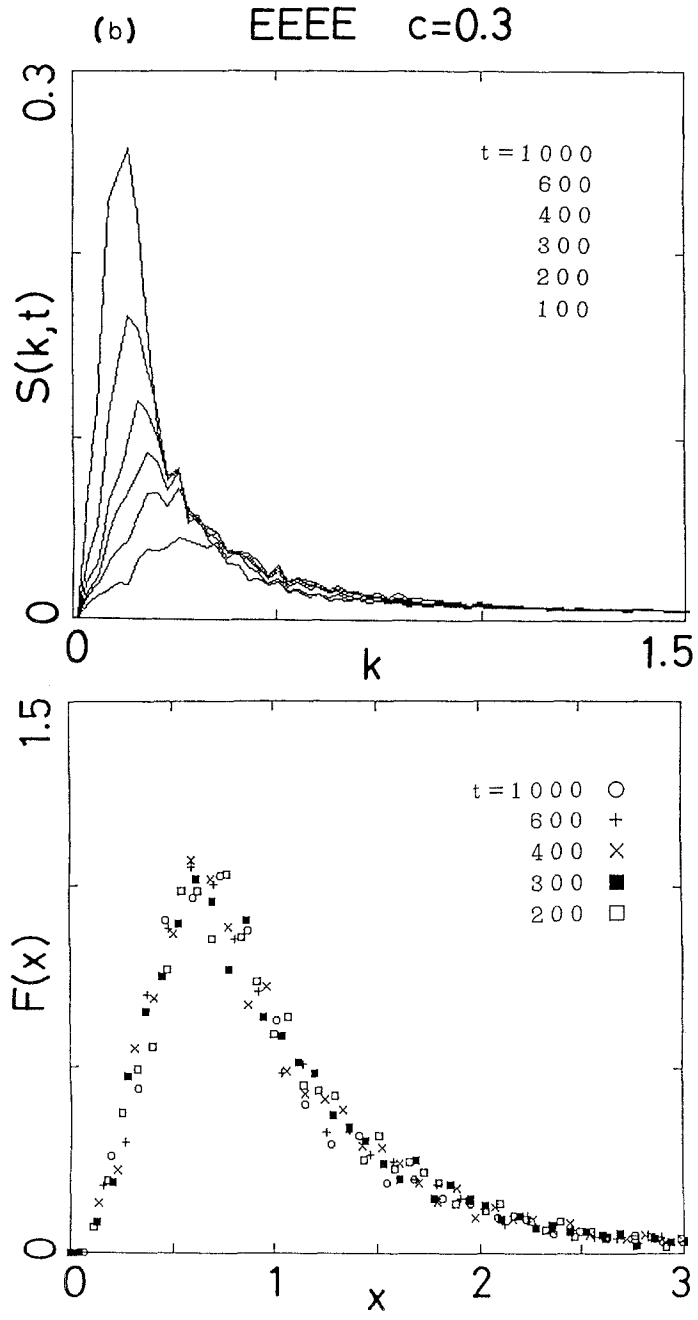

Fig. 11. (*Continued*)

where $S_{crit}(k)$ is the structure function for the critical concentration for cluster growth and k_c is a cutoff wave number. As a characteristic wave number, we define the mean wavelength, i.e.,

$$\langle k(t) \rangle = \sum_k kS_1(k, t) \Big/ \sum_k S_1(k, t) \tag{7}$$

Using these quantities, we define a normalized scaling function

$$x = k/\langle k(t) \rangle$$

$$F(x, t) = L/\pi \langle k(t) \rangle^2 S_1(k, t) \Big/ \sum_k kS_1(k, t) \tag{8}$$

If the scaling assumption is satisfied, the function $F(x, t)$ does not depend on time t.

We show the numerical results for $S(k, t)$ and $F(x)$ in Fig. 11. In every case, we have averaged over 30 samples with different initial configurations in a 128×128 lattice space. For the rule 01FF, while the critical concentration is assumed as $c_{crit} = 0.22$, $c_{crit} = 0.65$ for rule EEEE. The figures indicate that the dynamical scaling is approximately attained in a certain time duration for every case. To obtain the scaling functions, we exclude very early times because there the initial distribution affects the dynamics, and very late stages, where finite-size effects become important. We expect that the dynamical scaling character can be observed over a longer time if the system size is increased.

4. DISCUSSION

In the cluster growth under the rule 01FF, elementary processes are adhesion and evaporation of particles, and the rate of adhesion to a large cluster exceeds a little that of evaporation from the cluster. Therefore larger clusters grow slightly faster than smaller clusters and finally only one largest cluster survives. In the case of the rule EEEE, on the other hand, activity of the cluster surface is the cause of cluster movement and deformation. Thus, cluster growth is caused by collision of neighboring clusters in the course of cluster deformation. The mechanism can be examined by changing the automata rule; too much activity of the surface puts the system in an almost gas phase and low activity induces no cluster growth. From these facts, we think that the dynamical scaling is attained according to the subtle balance of adhesion and evaporation for the rule 01FF and according to a degree of surface activity for the rule EEEE.

Since the dynamics defined in Section 2.3 is one of many possibilities,

other dynamics may generate different pattern and time characters. But in several examples that we have examined numerically the asynchronous dynamics using random selection of pairs have the same pattern characters as that of the synchronous dynamics we have studied, but the temporal behavior of these two models is different. The details will be clarified in another paper.

ACKNOWLEDGMENTS

The author would like to thank Y. Aizawa and P. Davis for fruitful discussions and encouragement.

REFERENCES

1. S. Wolfram, *Rev. Mod. Phys.* **55**:601 (1983).
2. G. Y. Vichniac, *Physica* **10D**:96 (1984); T. Toffoli, *Physica* **10D**:117 (1984); T. Toffoli and N. Margolus, *Cellular Automata Machines* (MIT Press, Cambridge, Massachusetts, 1987).
3. U. Frish, B. Hasslache, and Y. Pomeau, *Phys. Rev. Lett.* **56**:1505 (1986); J. B. Salem and S. Wolfram, in *Theory and Application of Cellular Automata*, S. Wolfram, ed. (World Scientific, Singapore, 1986), p. 362.
4. Y. Pomeau, *J. Phys. A: Math. Gen.* **18**:L415 (1984); M. Cruetz, *Ann. Phys.* **167**:62 (1986).
5. Y. Pomeau and G. Y. Vichniac, *J. Phys. A: Math. Gen.* **21**:3297 (1988).
6. S. Takesue, *Phys. Rev. Lett.* **59**:2499 (1987).
7. T. Kohyama, *Prog. Theor. Phys.* **81**:47 (1989).
8. A. Rucklidge and S. Zaleski, *J. Stat. Phys.* **51**:299 (1988).
9. K. Kawasaki, in *Phase Transitions and Critical Phenomena*, Vol. 2, C. Domb and M. S. Green, eds. (Academic Press, London, 1972), p. 443.
10. J. Hardy, Y. Pomeau, and O. de Pazzis, *J. Math. Phys.* **14**:1746 (1973); J. Hardy, O. de Pazzis, and Y. Pomeau, *Phys. Rev. A* **13**:1949 (1976).
11. J. D. Gunton, M. San Miguel, and P. S. Saint, in *Phase Transitions and Critical Phenomena*, C. Domb and J. L. Lebowitz, eds. (Academic Press, London, 1983); J. L. Lebowitz, J. Marro, and M. H. Kalos, *Acta Met.* **30**:297 (1982); Y. Oono and S. Puri, *Phys. Rev. Lett.* **58**:836 (1987).